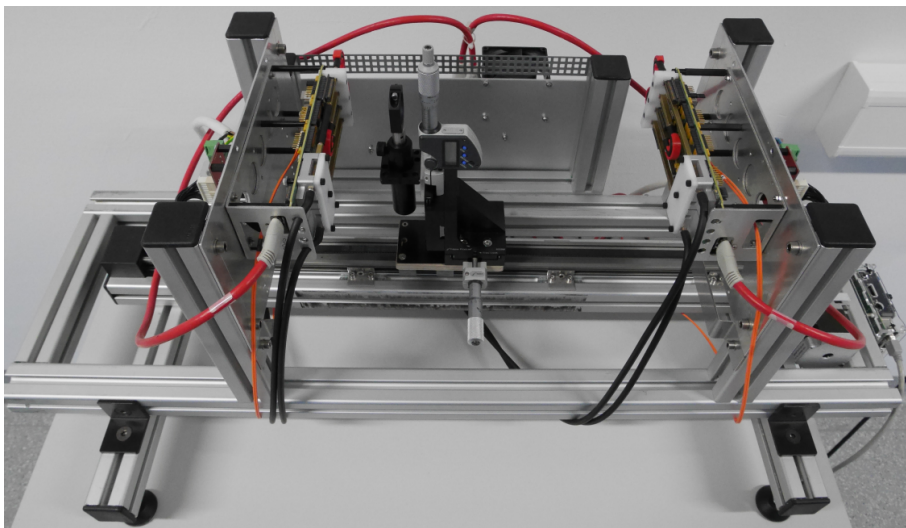


Advanced lab course for Bachelor's students

M21 Medical physics

Positron Emission Tomography (PET)



January 2020
Karl Krüger, email: karl.krueger@pmi.rwth-aachen.de

Prerequisites:

- Interaction of γ -rays and matter
- Scintillators
- Photo diodes, p-n-junctions
- Radiation detection

Aims of this experiment:

- Detector electronics
- Digital Silicon Photo-Multipliers (dSiPMs)
- Determination of detector characteristics
 - Energy resolution
 - Timing resolution
 - Detector sensitivity

Contents

1 Preface	5
2 Theoretical Background	6
2.1 Principle of PET imaging	6
2.2 Detection of gamma-photons by silicon photomultipliers	7
2.2.1 Scintillators for PET imaging	7
2.2.2 Photodetectors	10
2.2.3 Single and coincidence processing	13
2.3 PET scanner characteristics	14
2.3.1 Energy resolution	14
2.3.2 Timing resolution	17
2.3.3 Sensitivity	18
3 Setup and Procedure of the Measurements	20
3.1 Setup	20
3.1.1 General Setup	20
3.1.2 Power Supply and Cooling	20
3.1.3 Sensor board	22
3.1.4 Start-up Procedure	22
3.2 Procedure of the experiments	24
3.2.1 General remarks	24
3.2.2 Calibration of the motorized linear stages	25
3.2.3 Basic Start-Up	25
3.2.4 Basic Shutdown	26
3.2.5 Determination of a dark count map	26
3.2.6 Count rate determination	27
3.2.7 Energy spectrum	28
3.2.8 Timing resolution and determination of source position by Time-of-Flight measurement	29
3.3 Analyzing your data	30
Bibliography	31
A Appendix	34
B Instructions	35
B.1 Overview of PET-scanner Procedures	35

B.2	Motor controls	36
B.2.1	Group 1: Dark box setup	36
B.2.2	Group 2: Open setup with shielded modules	37

1 Preface

Aim of this lab course is to show the principle of positron emission tomography (PET) imaging and how digital Silicon-Photomultipliers (dSiPM) are used in this application. You will perform experiments to determine the sensitivity as well as the energy and timing resolution as important characteristics of a PET scanner. Measurements are performed on a simple PET scanner consisting of two detector elements, measuring γ -events of a ^{22}Na -point source.

These instructions are organized as follows: In the first two sections the principle of PET imaging (2.1) and gamma detection with (digital) SiPMs (2.2) are briefly described. In Section 2.3 the PET scanner characteristics measured in this lab course are explained, as well as their influence on imaging.

The experimental setup and procedure are delineated in sections 3.1 and 3.2. Finally, instructions for the data analysis are given in Section 3.3.

The experiment will be conducted in the rooms of the department of Physics of Molecular Imaging Systems (PMI) at the Zentrum für Bio-Medizintechnik (ZBMT), first floor, Pauwelstr. 17, 52074 Aachen. Please ring the bell of the PMI institute at the front door to enter the ZBMT.

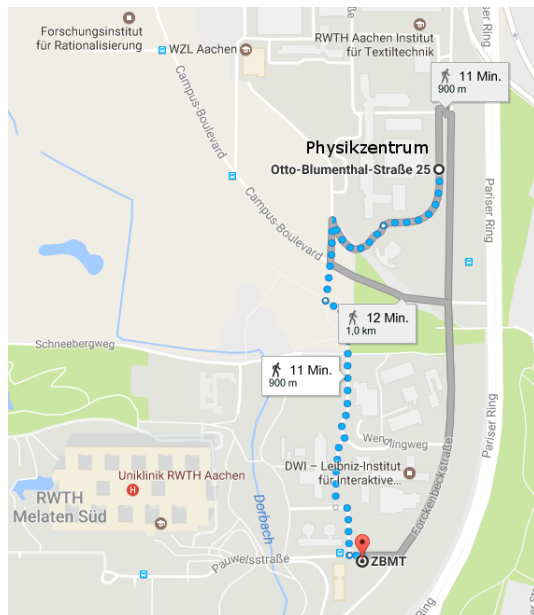


Figure 1.1: Directions to ZBMT Aachen, ([Google Maps link](#)).

2 Theoretical Background

2.1 Principle of PET imaging

In contrast to computed tomography (CT) and magnetic resonance imaging (MRI), both imaging patient's anatomy, the aim of positron emission tomography (PET) is to show metabolic functions. Figure 2.1 gives an overview of the molecular sensitivity (lowest concentration of an imaged agent that can be accurately detected in a medium) and spatial resolution of different imaging modalities.

In PET, a small amount of a radioactively-labeled chemical compound (so-called tracer) is injected in the patient. The tracer allows imaging of the desired metabolic process, e.g., glucose uptake of tumor cells to identify cancer metastasis. PET aims at imaging the spatial and temporal distribution of the tracer, showing the biological process(es) and ideally also allowing quantification, e.g., to evaluate therapy response. Clinically, it is used mainly in the fields of oncology, cardiology and neurology, e.g., for the diagnosis of Alzheimer's disease.

Tracers for PET imaging are positron emitters like ^{18}F -fluorodeoxyglucose (FDG) and ^{82}Rb -chloride. The emitted positron deaccelerates until it either annihilates directly with an electron or after forming a bound state with an electron (called positronium). In both cases, the annihilation most probably results in two γ -photons of 511 keV emitted back to back (at an angle of 180°) in the center-of-mass frame. Emission of three photons is also possible, but unlikely (<1%).

What angles between the two γ -photons, are observed in the lab frame?

Ideally, the emitted γ -photons travel through the patient and are detected by the PET-detector surrounding the patient. The points of detection define a so-called line of response (LOR), on which the annihilation has occurred (see Figure 2.2(a)). By measuring a large amount of these LORs, the original tracer distribution can be calculated (see Figure 2.2(b)). The calculation of the underlying tracer distribution from the detected events or LORs is called (image) reconstruction. Frequently used reconstruction methods are filtered back-projection or maximum likelihood expectation maximization. More information regarding image reconstruction methods can be found in [3, 4, 7].

By measuring the time difference between the detection of the two γ -photons, the point of annihilation can be limited to a smaller section along the line of response and ideally to a single point (see Figure 2.3). The width of the time difference distribution of a point-like source is called coincidence resolving time (CRT), usually displayed as full width at half maximum (FWHM). Nowadays, the CRT of (pre-)clinical PET systems is in the order of 200-500 ps. The timing uncertainty is

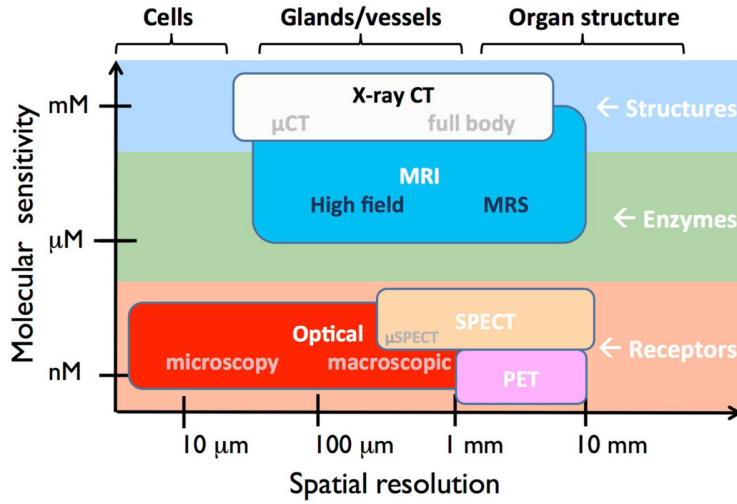


Figure 2.1: Comparison of medical imaging modalities with respect to molecular sensitivity and spatial resolution, from [9]

mainly caused by the scintillation process and statistical uncertainties of detecting the optical photons, but also timing jitter of the electronics contributes to the CRT (about 20 ps). In this lab course, the timing resolution of the PET scanner will be measured and used to determine the unknown position of a point source.

2.2 Detection of gamma-photons by silicon photomultipliers

2.2.1 Scintillators for PET imaging

In PET imaging, the γ -photons are usually detected in a two-staged process. First, a γ -photon is converted to a large number of optical or ultraviolet photons by scintillation. In a second step, these optical photons are detected by photosensors. Since the principle of scintillation is already described in the instructions of the lab course T1 [1], it is not repeated here. Instead, the properties of scintillators that are important for PET imaging are delineated.

Attenuation coefficient at 511 keV. The linear attenuation coefficient is the fraction of attenuated incident photons per unit thickness of a material. A high attenuation coefficient at 511 keV reduces the probability that the γ -photon passes the scintillator without depositing (its total) energy and the photon potentially leaves undetected or is detected with a wrong energy value. The attenuation coefficient is dependent on the energy of the γ -photon.

Intrinsic energy resolution is a lower bound for the detector energy resolution (see Section 2.3.1). Energy resolution is important to distinguish between

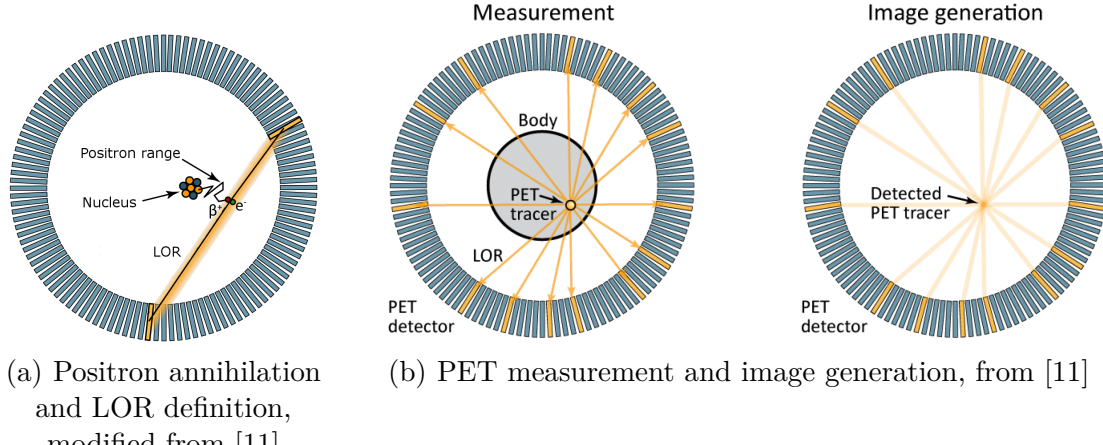


Figure 2.2: Visualization of PET imaging principle.

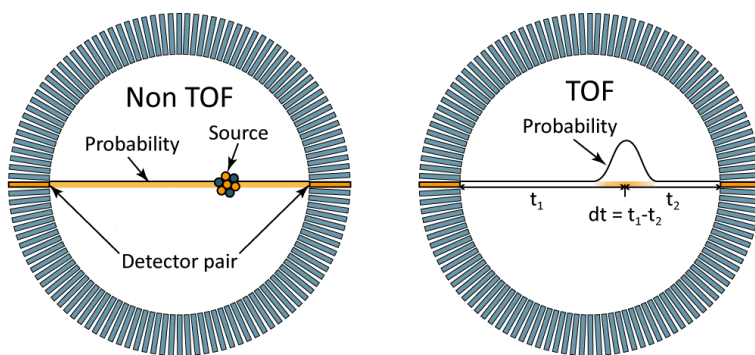


Figure 2.3: Visualization of the Tof-PET principle, modified from [11]

γ -photons emitted at the point of annihilation and those that have been scattered (e.g. by Compton scattering in the patient). Scattered photons partly lose the information about the annihilation point and lead to false LORs, causing additional noise in the reconstructed image. The role of energy resolution and effects of scatter are described in more details in Section 2.3.1. To achieve a good energy resolution, a high light output with a small variation in the number of produced optical photons per energy is required.

Fast emission of photons is required to allow an exact time stamping of the energy deposition in the scintillator, which is needed to allow time-of-flight measurements. Furthermore, a short decay time reduces the probability that scintillation processes of multiple γ -photons pile-up, resulting in a difficult or impossible determination of the number of incident γ -photons.

Scintillator materials commonly used in PET imaging are crystals of bismuth germanium oxide ($\text{Bi}_4\text{Ge}_3\text{O}_{12}$, BGO) or cerium-doped lutetium yttrium orthosilicate ($\text{Lu}_{1.8}\text{Y}_{0.2}\text{SiO}_5(\text{Ce})$, LYSO). The relevant properties of BGO, LYSO and for com-

parison also the properties of sodium iodide (NaI) are given in Table Table 2.1.
LYSO contains lutetium, which is intrinsically radioactive. Does this affect the measurements?

Parameter	NaI	BGO	LYSO
Effective Z	50.6	73	65
Density / (g/cm ³)	3.67	7.13	7.1
Peak emission / nm	410	480	420
Light output / ph.	19400	4200	~ 16000
Intrinsic $\Delta E/E(\%)$	5.8	3.1	~ 9
Decay time / ns	230	300	~ 40
Index of refraction	1.85	2.15	1.8
Attenuation coefficient / (cm ⁻¹)	0.34	0.96	0.82
Attenuation coefficient @1275 keV / (cm ⁻¹)			0.39

Table 2.1: Scintillator properties, if not stated otherwise, for a gamma energy of 511 keV. The properties largely depend on the exact doping and production of the scintillators and are not to be taken as exact values (taken from [6]).

The optical photons emitted in the scintillator have to traverse and leave the scintillator material to be detected by the photosensors. Therefore, the scintillator has to be transparent for these photons and total reflection at the boundary surface of the scintillator and the photodetector has to be avoided. Hence, the refractive index of the scintillation material is an important property as well.

Regarding the assembly of scintillator material in PET detectors, there are three options (see Figure 2.4):

One-to-one coupling The scintillator material is cut in blocks with a base area equal to the photodetector elements' base area and is directly aligned and glued on top, so that one photodetector element is coupled to one scintillator 'pixel'. This is the simplest configuration, but it is only feasible for relatively large scintillator pixels of a few millimeters.

High-resolution scintillator In this configuration, the scintillator elements have a much smaller base area than the photodetector elements. The optical photons are distributed to the photodetectors via an extra layer (so-called light guide). The light guide spreads the light of a scintillator element to multiple photodetector elements. Therefore, several photodetector elements have to be read-out and a positioning algorithm is required to determine the crystal hit by the γ -photon (see Figure 2.5).

Monolithic crystal For a monolithic crystal, the position of the interaction of the γ -photon with the scintillator material has to be reconstructed from the ph-

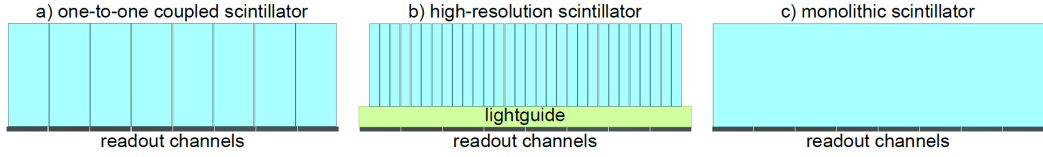


Figure 2.4: Scintillator crystal configurations, from [6]

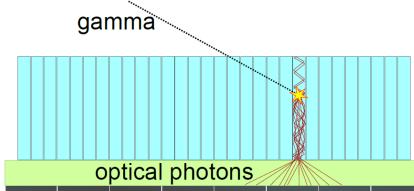


Figure 2.5: Sketch of a high resolution scintillator configuration, [6]

todetector signal. This requires knowledge of the correlation of the scintillation position and the measured signals, which has to be derived by calibration measurements.

2.2.2 Photodetectors

For the detection of the optical photons emitted by the scintillator, two different kinds of detectors are commonly used: Photomultiplier tubes and semiconductor-based sensors. Here, we focus on semiconducting photosensors, particularly digital Silicon-Photomultipliers (dSiPM).

To explain the principle of a dSiPM, we introduce a photodiode as the basic implementation of a semiconductor-based photosensor. First, we consider a photodiode as a simple p-n-junction. More information on p-n-junctions and their properties can be found in the instructions of T1 [1].

If a photon with a sufficient energy (higher than the band gap) hits the depletion zone, an electron hole pair is created. Due to the intrinsic voltage the electron travels to the cathode (n-doped layer), while the hole travels to the anode (p-doped layer), resulting in a so-called photo-current. To increase the (sensitive) depletion zone, an additional low-doped layer (so-called the intrinsic region) is often incorporated between the p- and n-layers resulting in a so-called PIN-diode (see Figure 2.6).

By applying a reverse bias voltage, the depletion width is increased while the response time of the diode is reduced. However, the reverse bias also results in a temperature dependent leakage current which is present even in the absence of light (dark current).

If the reverse bias voltage is below the breakdown voltage, the photocurrent is proportional to the number of absorbed optical photons and only slightly depending on the bias voltage. However, since each photon creates only a single electron-hole pair, the photocurrent is very small.

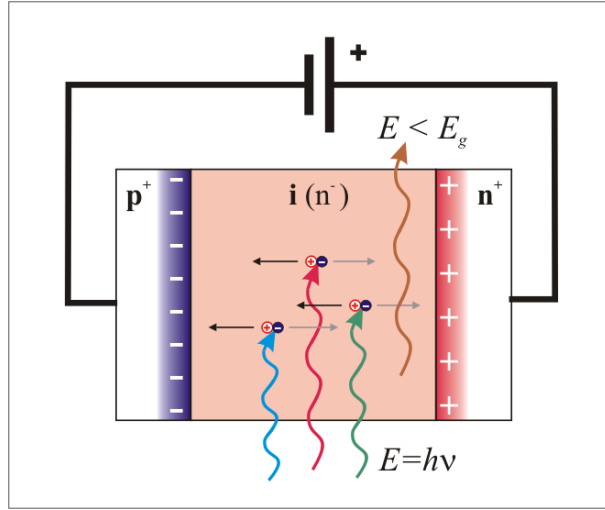


Figure 2.6: PIN-photodiode with space charge distribution under reverse voltage.
 (@User:Kirnehkrib/Wikimedia Commons/ [cc-BY-SA 3.0](#))

For bias voltages higher than the breakdown voltage, each free charge carrier in the depletion zone induces an avalanche of charged particles. The rise time of the resulting signal is in the order of a few picoseconds and due to the internal gain, the photocurrent is much higher compared to the current in a PIN-diode. However, in this so-called Geiger mode¹, the avalanche is the same for every event and no longer proportional to the number of incident photons. Therefore, such a device, called single photon avalanche diode (SPAD), delivers a binary signal if a photon is detected.

Since the avalanches in a SPAD are self-sustaining, quenching is required to reset a SPAD after photodetection. For quenching, the bias voltage has to be reduced below the breakdown voltage. This can be done passively by a high ohmic resistor in series with a SPAD. The photocurrent leads to a voltage drop at the resistor reducing the bias voltage below the breakdown voltage and hence stopping the avalanche. After quenching, the bias voltage recovers. This recovery process takes about a few nanoseconds and during this period no further photons can be detected. To reduce this SPAD dead time, the bias voltage can also be reduced actively by electronics (active quenching). In this case the SPAD has to be reset by ramping-up the bias voltage again to make the SPAD sensitive for the next photon.

To build a useful photocounting sensor, a Silicon-Photomultiplier (SiPM), multiple small area SPADs (also known as microcells) are combined and connected in parallel (see Figure 2.7). The photocurrents of the SPADs add up to a signal from which the number of detected photons can be recovered by pulse height or shape analysis (see Figure 2.8). Thus, the optical photon shower created in the scintillation process from a single γ -photon can be detected.

The digitization and time stamping of the analog SPAD signals is done by an

¹The name is inspired by the analogy to the Geiger Müller counter

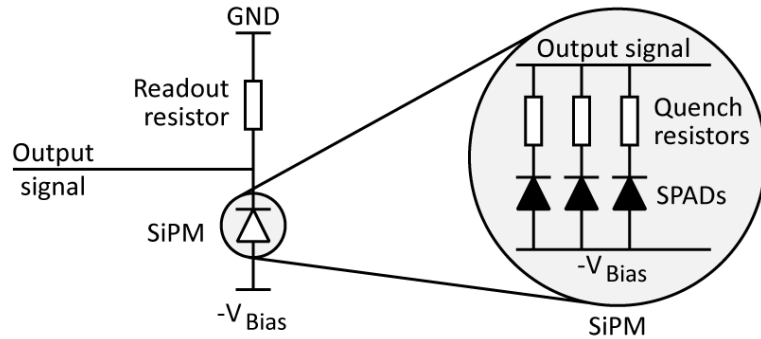


Figure 2.7: SiPM circuits: An SiPM is constructed from SPADs in series with individual quench resistors, connected in parallel (right). In series with a readout resistor, they produce an analog output signal. Taken from [11].

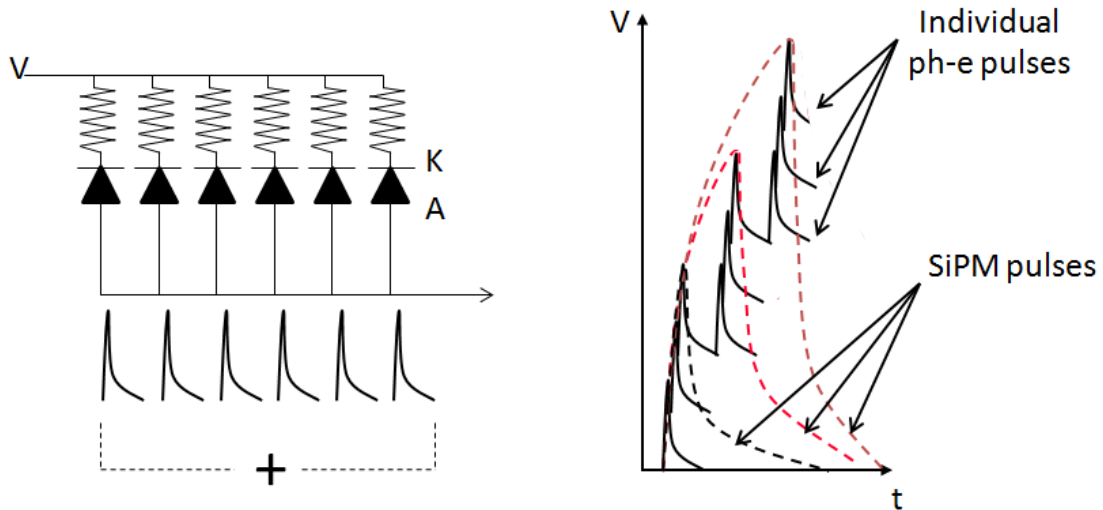


Figure 2.8: Left: Schematic of the equivalent electrical circuit of a SiPM. Only 6 micro-cells, each represented by a diode symbol, are shown. Right: Illustration of the signal formation in a SiPM. The pile-up of the individual micro-cell pulses is achieved by means of summing via a common readout line. (reprinted from [8] 3.0).

application-specific integrated circuit (ASIC). Figure 2.9 shows a light detection system consisting of SPADs and a ASIC-based readout electronics.

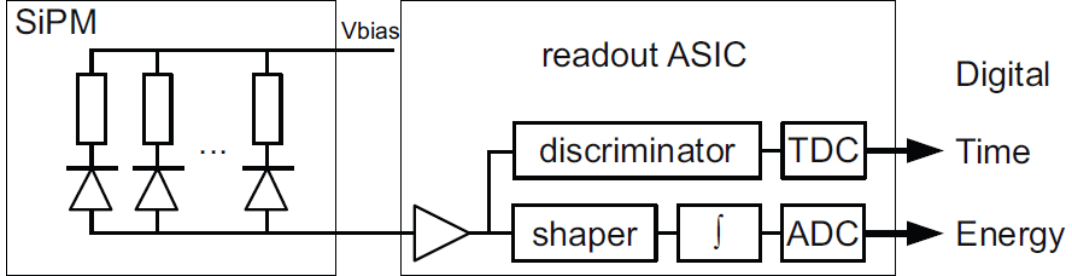


Figure 2.9: Scintillation light detector systems based on an analog silicon photomultiplier. (reprinted from Frach et al. [2], ©IEEE)

In digital SiPMs (dSiPMs) each SPAD signal is digitized, transforming a single SPAD into a digital device that can detect a single photon. These digital signals are more robust than the analog-signal-summation in analog SiPMs, which is prone to temperature-induced gain changes and usually requires compensation.

The digital SPAD is actively quenched and stays in this state until it gets recharged. During quenching, further photons cannot be detected. Thus, the output signal relates to a single photon. The digital sum of these signals represents the number of photons recorded. When an optical photon shower is recorded by a digital SiPM, the SPAD sum is sent out together with the timestamp of the earliest photons detected in a digital format.

The active quenching circuit of individual SPADs allows to characterize SPADs individually in terms of their noise behavior. To measure the dark count rate on SPAD level, a single SPAD per dSiPM is activated at a time and the count rate of the dSiPM is evaluated and can be attributed to the activated SPAD. This allows to deactivate a certain fraction of SPADs based on their dark count rate which sacrifices photon sensitive area of a dSiPM at the gain of a reduced overall dark count rate (see Section 3.2.5).

The increased robustness is particularly interesting for the combination of PET detectors and MRI, since the inside of an MRI poses a harsh environment for electronics due to the strong static magnetic field and potential induction of high voltages by time-varying magnetic fields.

2.2.3 Single and coincidence processing

The dSiPMs are self-triggering devices. When a photon shower is detected a digital hit containing a timestamp and the number of detected photons is sent out and captured by the readout electronics. On a detector block which often employs many dSiPMs these hits are correlated based on their timestamp. From this cluster of digital hits the information of the corresponding interaction of a γ -photon in the

scintillator is deduced. In PET this is called a single. As described in Section 2.1, two coincident events or singles are required to determine the LORs needed for reconstruction of the tracer distribution. Hence, the individual singles have to be checked for coincidence with other events. For this purpose, a sliding coincidence window is used to find coincident singles. Only coincidences of exactly two singles are accepted, others are rejected.

2.3 PET scanner characteristics

The scanner characteristics covered in this lab course are: energy resolution, timing resolution and detection probability. In the following these characteristics, their influence on imaging and how they can be measured are delineated.

2.3.1 Energy resolution

The 511 keV γ -photons traveling through the patient interact with patient's tissue mainly via the mechanisms of the photoelectric effect and Compton scattering. Since the mean free path of 511 keV in water is about 70 mm, in clinical applications many γ -photons were scattered before being detected by the PET detector. Compton scattering alters the energy and direction of the scattered photon, therefore scattered photons lead to wrongly assumed LORs resulting in background noise in the image (see Figure 2.10).

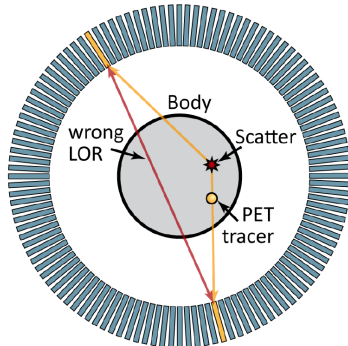


Figure 2.10: Scattered γ -photons result in wrongly assumed LORs that increase the image background noise, from [11]

By filtering these scattered photons by their reduced energy, this background noise can be avoided or reduced. However, the limited energy resolution broadens the photopeak at 511 keV and depending on the energy resolution an energy window of sufficient width has to be chosen to preserve a sufficient sensitivity. In Figure 2.11 measured energy spectra of a ^{22}Na source are depicted. Figure 2.11(a) shows the spectrum of detected singles while Figure 2.11(b) shows the spectrum of single events that are in coincidence with another event. The energy resolution of a PET

scanner is usually defined by the FWHM of the 511 keV photopeak over the energy. To evaluate the role of energy resolution, the relation between maximum scatter angle and energy resolution can be derived from Compton formula (Equation 2.1) and is plotted in Figure 2.12.

$$E'_\gamma = \frac{E_\gamma}{1 + \frac{E_\gamma}{m_0 c^2} (1 - \cos \theta_c)} \quad (2.1)$$

Here, E_γ is energy of the incident photon, E'_γ is the energy of the photon after the scattering process, m_0 is the rest electron mass, c is the speed of light and θ_c is the scattering angle.

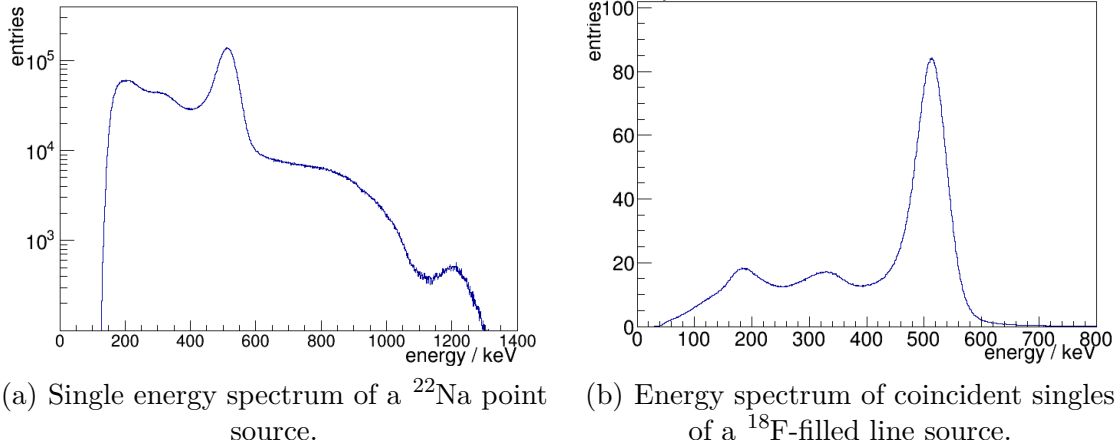


Figure 2.11: Energy spectra of singles and coincident singles, from [6]

To measure the energy resolution of the PET-detector an energy calibration has to be performed first (see [6] for detailed information). After calibration a spectrum of coincident singles is acquired and the energy resolution can then be derived by fitting a Gaussian distribution to a suitable part of the photopeak. The linearity of the calibration can be checked by the second photopeak of ^{22}Na at 1275 keV acquired in the energy spectrum of all singles.

Besides scatter inside the patient, what other processes can cause detection of γ -photons with less than 511 keV?

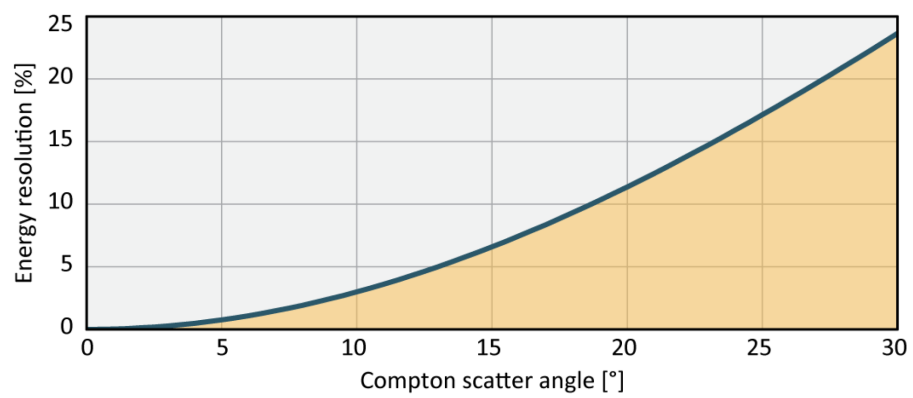


Figure 2.12: Energy resolution that is needed to detect that a 511 keV γ -photon was Compton-scattered, over the scatter angle (and respectively: the Compton scatters that can be detected, relative to the energy resolution). Taken from [11]

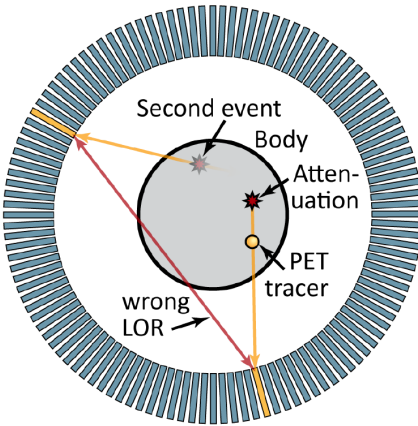


Figure 2.13: Random coincidence: Two single γ -photons of different events (the others are e.g. attenuated or the second event was outside the FOV) are detected simultaneously as a wrong LOR.b Taken from [11]

2.3.2 Timing resolution

To combine detected single γ -photons to coincident events, a sliding time window is used to group singles to coincidences. The size of this coincidence window (CW) has to be chosen large enough to allow the γ -photons to travel through the complete distance between the detectors plus a safety margin depending on the timing resolution of the detector. On the other hand a large CW can result in the situation that γ -photons of different annihilations are falsely grouped to coincidences. Considering an example with two annihilations in a CW, the following cases are possible:

More than two photons detected: In this case the events either have to be discarded, or further processing is required to find the most probable LOR(s), which can lead to wrong LORs.

Two photons detected: If only two photons originating from different positron decays are detected with their respective counterpart not being detected by the PET or stopped in the patient, one cannot distinguish this situation from detecting a true coincidence, therefore a wrong LOR is assumed in this case. These events are called randoms and induce background noise to the image. Fig 2.13 illustrates the situation for random events. The rate of random events is approximately proportional to the length of the coincidence window and the singles rates.

Timing resolution of a PET scanner can be determined by acquiring a time difference histogram of a point source and fitting a Gaussian distribution to it (see Figure 2.14). Usually the timing resolution is reported as the FWHM of the fitted Gaussian distribution.

If the timing resolution is smaller than the time that the γ -photons need to pass the distance between the detectors, time-of-flight (ToF) measurements become useful.

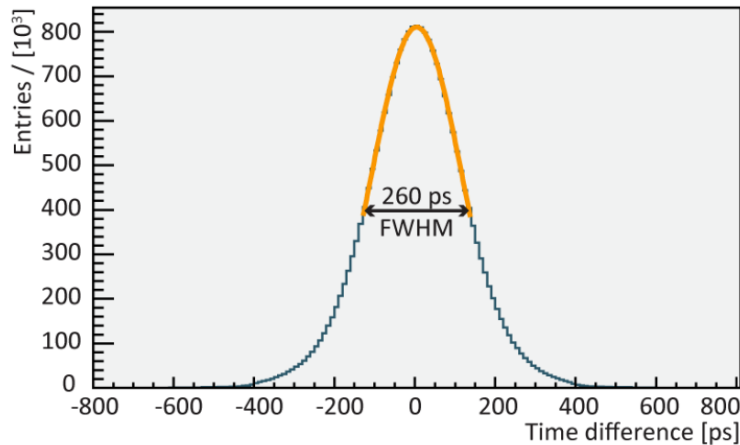


Figure 2.14: Timing resolution measured with the Hyperion-IID PET-insert using timing-optimized settings. A single ^{22}Na point source (1.3 MBq) was placed in the center of the FOV for the scan. Taken from [11]

In this case the timing difference can be used to limit the LORs to smaller sections and ideally to a single point (see Figure 2.3). In reality, the timing resolution is in the order of 200-500 ps FWHM, so the probable area of annihilation along the LOR can be limited to a length of 6-15 cm. ToF imaging results in less noise and therefore a better contrast in the images.

In this lab course you will determine the unknown position of a point source by a time of flight measurement.

Make a rough estimation of the error of this measurement. (To determine the position you can measure many coincidences originating from the point source.)

2.3.3 Sensitivity

The sensitivity of a PET scanner is here defined as the fraction of radioactive decays that are detected by the system (number of coincidences) over the decays of the tracer or radioactive source. The sensitivity depends on a number of factors:

Geometric Efficiency Only those γ -photons that pass the scintillating material at least partly have the chance to deposit energy in the scintillator and to be detected. Accordingly, the geometric efficiency is defined as the solid angle covered by the detector arrangement that allows to measure coincident singles. The geometric efficiency is often calculated for the iso-center assuming a point source or has to be integrated for a certain volume and a distributed tracer.

Detection Efficiency Even if a γ -photon travels through the scintillator, it might not deposit (part of its) energy and leave undetected. A scintillator material with high attenuation (at 511 keV) as well as larger scintillators can reduce

the rate of undetected γ -photons. However, large scintillators induce other problems in PET imaging.

What problems can be caused by large scintillator crystals?

Sensor Dead Time If a photo sensor and the digitization circuit or the dSiPM is busy acquiring a photon shower or it was triggered by noise and has to be reset, a consecutive photon shower might not be detected. This sensor dead time is dependent on the noise and thus the temperature and its influence on the sensitivity depends on the rate of photon showers.

Is this the dominant dead time or could other factors contribute to the system dead time as well?

3 Setup and Procedure of the Measurements

3.1 Setup

3.1.1 General Setup

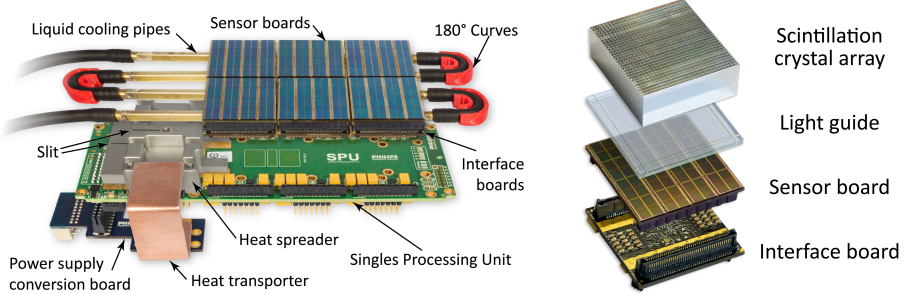
For the experiments, two slightly different setups are used. In both cases, the actual detector consists of two module boards, called singles processing unit (SPU) (see Figure 3.1(a)). The SPUs can hold up to six detector stacks. In the current experiment two of these stacks are mounted per SPU. A detector stack consists of an interface board, the actual sensor board and a scintillator mounted on top (see Figure 3.1(b)). The SPUs are responsible for controlling the sensor boards, e.g. enabling or disabling SPADs or ramp-up of the bias voltage. In addition, they manage the data transmission of PET data to the data acquisition and processing server (DAPS). The SPUs are mounted on brackets of aluminum profiles screwed to a base frame. In the one setup, the SPUs are additionally placed in light-tight casings to prevent ambient illumination that disturbs the PET measurements. In the other setup, the whole frame is placed inside a dark box together with a third module board (so-called backbone), that provides sync and reference clock to the SPUs. These signals are conducted via HDMI connections between each SPU and the backbone. Fig. 3.2 depicts the latter setup outside the dark box.

In this experiment, a ^{22}Na source is used. Please note that for ^{22}Na , other than the explained decay process may be possible. The point source is mounted on a carriage adjustable in 3 dimensions (Figure 3.3). The movement along the axes is either controlled by stepper motors connected to controllers or manual translation stages. For the time-of-flight (ToF) measurements, the source has to be shifted between the two SPU frames using the linear translation stages. The data-sheet of the ^{22}Na point source can be inspected at the day of the experiment.

The different components (DAPS, SPUs, backbone, stepper) are controlled via a system-control software (Hyperion, motor control software) on a separate control-PC. An introduction to the system software will be provided by the tutor at the beginning of the lab day.

3.1.2 Power Supply and Cooling

Each SPU requires three voltages for power (Low 1.9 V, Mid 3.0 V, High 4.9 V) as well as a Bias voltage of 30 V. The backbone requires the same voltages for power,



(a) Exploded-view photo of the SPU, detector stacks (without scintillator and light guide) and cooling infrastructure.

(b) dSiPM-based detector stack scintillation crystal array shown upside down to emphasize the individual crystals.

Figure 3.1: SPU and detector stack. Both images are taken from [10], 2015 IEEE

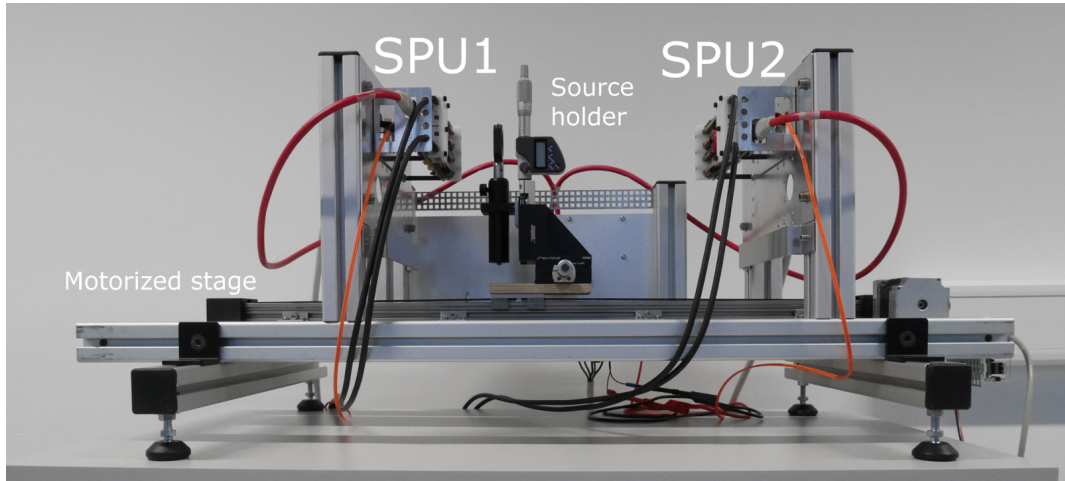


Figure 3.2: Setup of the experiment, the backbone module is located behind the aluminum plate at the backside. The dark box, power supplies, cooling unit, data acquisition and control PCs are not displayed.

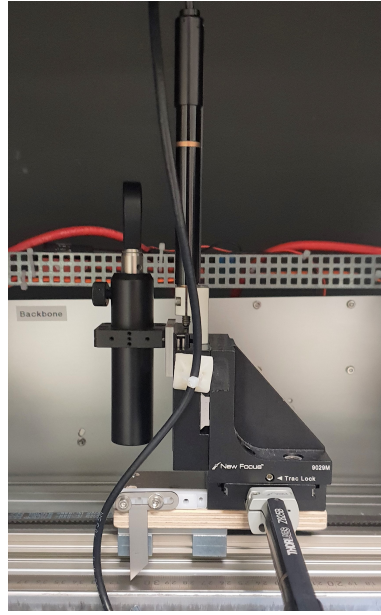


Figure 3.3: Source holder with motorized translation stages to adjust the source's position. The holder is mounted to a third stage to move the source holder between the detector modules.

but no additional bias voltage. These powers are supplied by a number of power supplies (dependent on the setup). The dark box setup is additionally equipped with a power supply that supplies the translation stages and their controller on the first line (24 V) and a fan (12 V) used for cooling the electronics of the backbone on the second line. The values on the power supplies should be preset as shown in Fig. 3.4(a) and should not be changed. If the values on the power supplies differ from the ones shown, inform your tutor before changing them.

The electronics of the detector SPUs and sensor boards are cooled by water cooling driven by a transportable process thermostat (Lauda).

3.1.3 Sensor board

The sensor boards are equipped with 16 sensor dies. Each of these dies has 2×2 dSiPM sensor channels that are connected via a single interface. The dSiPM-sensor channels (DPC 3200-22, Philips Digital Photon Counting, Aachen, Germany) consist of 3200 microcells (SPADs), each with a size of $59.4 \mu\text{m} \times 64 \mu\text{m}$. Figure 3.5 shows the structure of sensor dies. The scintillator crystals for the experiment are pixelated, one-to-one coupled LYSO arrays with dimensions of $32 \times 32 \times 12 \text{mm}^3$ each.

3.1.4 Start-up Procedure

The first start-up procedure should be performed together with the tutor.



(a) Power supplies for the dark box setup. The lower row shows the voltages for SPU 1 from right to left: Low, Mid, High, Bias. The middle row shows the voltages for SPU 2 from right to left: Low, Mid, High, Bias. The upper row shows the voltages for the Backbone from right to left: Low, Mid, High.

(b) Power supplies for the open setup. The lower row shows the voltages for SPU 1, the upper row for SPU 2. On the right is the Bias voltage, on the left Mid. Low is generated on the SPUs from the Mid voltage, High is generated on the 5V auxiliary port of the power supply.

Figure 3.4: Power supplies for both setups.

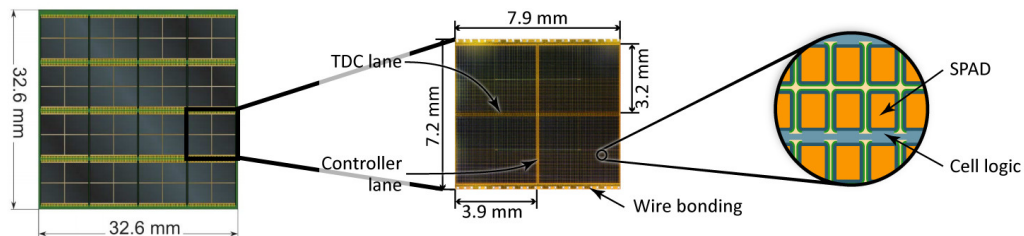


Figure 3.5: Sketch of a sensor board (left) with a zoom to a microscopic photo of a 2×2 dSiPM array (mid, also known as sensor die), followed by a magnified sketch (right) of the sensor structure, from [5] and [11]

Cooling Cooling should be started and running, before the SPUs are powered up. First, power up the process thermostat and set the target temperature to 15 °C. Check that the cooling fluid is circulating. Then power up the motor controller and the fan used to cool the electronics of the backbone module. Check that the fan is rotating.

Power up the SPUs Switch on the DC power supplies: Enable the three voltages supplying the backbone from Low to High. Wait for the backbone to boot (after a successful boot, the High voltage of the backbone should be around 1.3-1.4 V). This step can be omitted for the setup outside of the dark box. Enable the three voltages supplying the SPUs from Low to High. At last, switch on the bias voltage. In case a restart of the SPUs is required, switch off High and turn it on again. If the power up procedure of the SPUs is finished the blue status LEDs should switch off.

System start-up procedure A detailed step-by-step instruction can be seen in Sub-section 3.2.3.

3.2 Procedure of the experiments

Detailed instructions for the acquisitions will be provided at the day of the experiment. To save and copy your data for the analysis, please bring a USB-stick.

3.2.1 General remarks

- Do not power up the system without cooling (water cooling for SPU1 and SPU2, and fan for the backbone).
- Close the dark box before the bias voltage is ramped up (script 'RampUpVoltages' or 'StartUp-Continue')
- Before opening the dark box, lower the bias voltages (script 'EnableSaveVoltages') and check that the bias voltages are reduced to about 15V.
- Check bias voltages and IDDA (quench) currents after ramp up and ramp down ('EnableSaveVoltages'). Typical values for ramped down mode are 15 V bias voltage while during ramp up, the bias voltage reaches 25 V. IDDA needs to stay below the 100 mA current limiting.
- 'FrameCounters' can be checked with the 'ReadFrameCounterAtSync' command under SPUs and by sending a sync-pulse from the backbone ('Modules -> SyncPulseCfgUnit)
- Display plots by clicking the 'Change' option and reset the 'measurement interval'. Then, select the parameters that should be displayed.

- Pause histogram plots and refresh them if necessary to avoid memory pile up. The program may crash otherwise.
- The commands for the motor controller can be found in the appended Instructions.

3.2.2 Calibration of the motorized linear stages

Instructions for the stages can be found in the appended Instructions.

3.2.3 Basic Start-Up

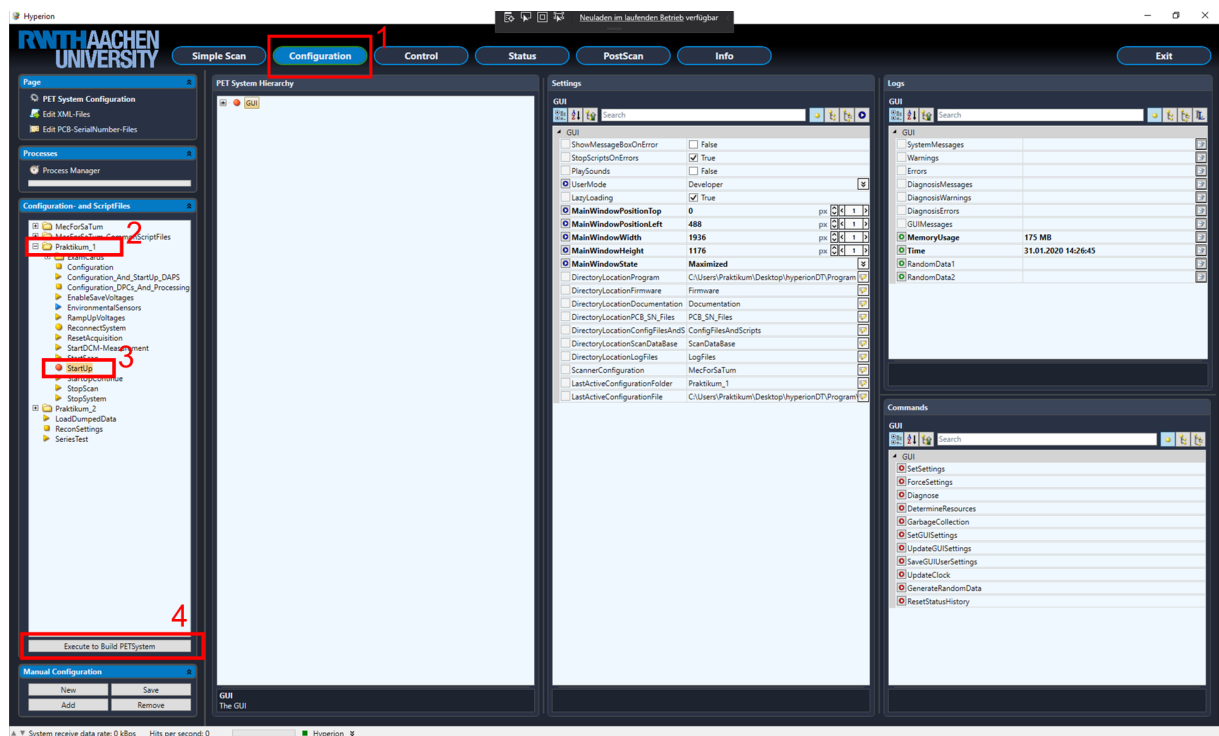


Figure 3.6: Hyperion Interface

- Start the Hyperion software (Fig. 3.6).
- Select the 'Configuration' tab (1) and open the 'Praktikum-X' configuration folder (2) on the left side (X: 1 or 2, number depending on the setup used) and execute 'Start Up' (select 3 and click 4).
- Check the 'Status' tab or the status bar at the bottom of the window. Check if the connection to the SPUs, the detector boards and the backbone are working

- Check that the system operates correctly in the 'Control' tab (bias voltage about 15V, temperatures of 'SPU' and 'SiPM', SPU power supply level).

3.2.4 Basic Shutdown

- Execute 'StopScan' if there is a scan running.
- Execute 'EnableSaveVoltages' to lower the bias voltage.
- Run 'StopSystem' and check status.
- Disable the power supplies in the opposite order and turn off the cooling systems.

3.2.5 Determination of a dark count map

A dark count map is a plot of the individual dark count rates of the dSiPM SPADs on a sensor board. To acquire such a dark count map, go to the 'Configuration' and select the coincidence unit. In our case the coincident unit is the DAPS-PC which will control the acquisition.

- Start up the system.
- Ensure that the dark chamber is closed.
- Execute 'RampUpVoltages' in the 'Praktikum_X' list to ramp up the bias voltage.
- Start the acquisition by executing the 'StartDCM-Measurement' command. The system will now measure the dark count rate for every SPAD and write it to a file.
- The current status can be seen under 'PETSystem -> SPUs -> [Select SPU]' in 'Logs' (right side). The counter is displayed in 'msg'.
- At the end of the acquisition, 'modus' will output 'finished' and write the file to the hard disk.
- Ask your supervisor to run the dcm tool and copy the resulting files from the DAPS to the Control PC.
- Check the files and save them to your USB-stick.
- Before starting normal measurements, restart the whole system.

Please note that only every second coordinate is listed, as the current DPCs consist of 3200 SPADs per pixel, and that the file needs to be processed before usage.

3.2.6 Count rate determination

- Start up the system.
- Execute 'Start-Up Continue'.
- Go to the 'Status' tab and check voltages, frame counters and temperatures on the SiPMs.
- Wait until the sensor tile temperatures (SiPM) stabilizes and note down the measured temperature of all 4 sensor boards.
- Execute 'StartScan'
- Use the translation stages of the source holder and the stepper motor (via the control software) to move the source to the position with the maximum count rate of coincidences. You can use the data rate plot (see Fig. 3.7) to find this position. Note here that one of the setups has one manual stage.

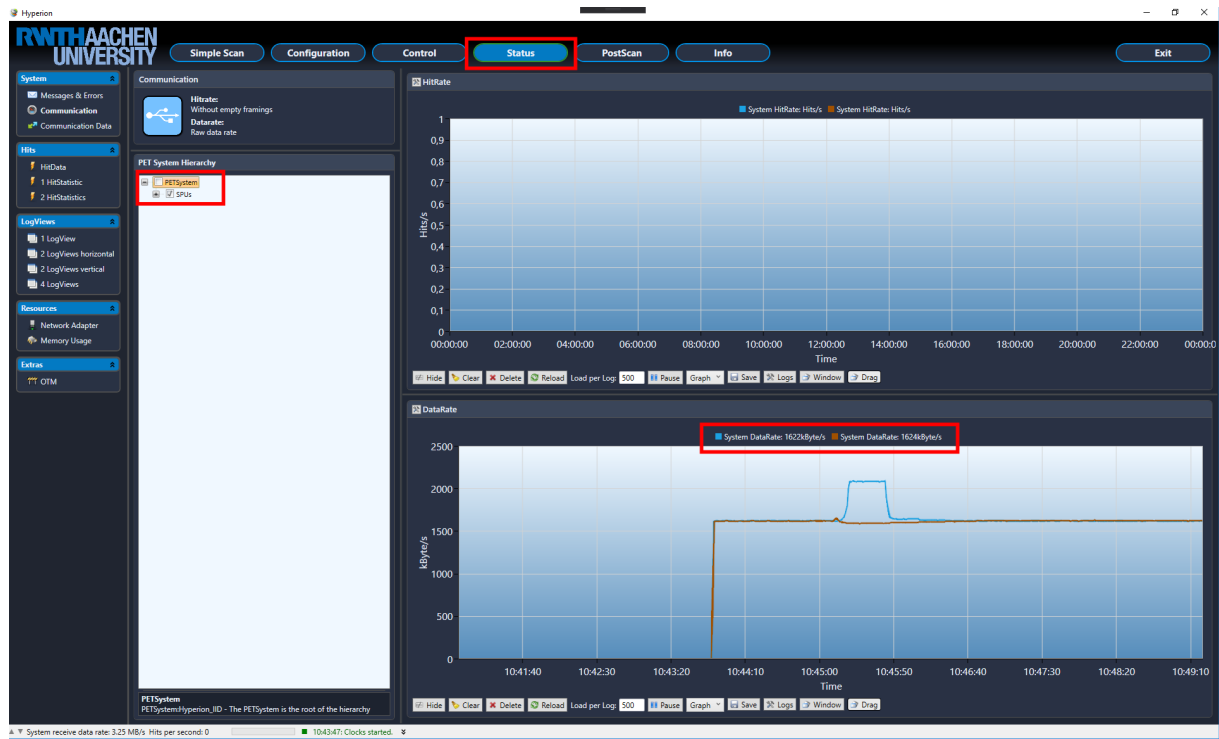


Figure 3.7: Hyperion data rate plot: Exemplary plot for the data rates of the two SPUs.

- Save the number of singles and coincidences at the found position to determine an average value in 'Coincidence Unit -> Modules -> DAPS Control', under 'Logs -> scpSingles' or 'Logs -> scpCoincidences' (see Figure 3.8 and 3.9). If

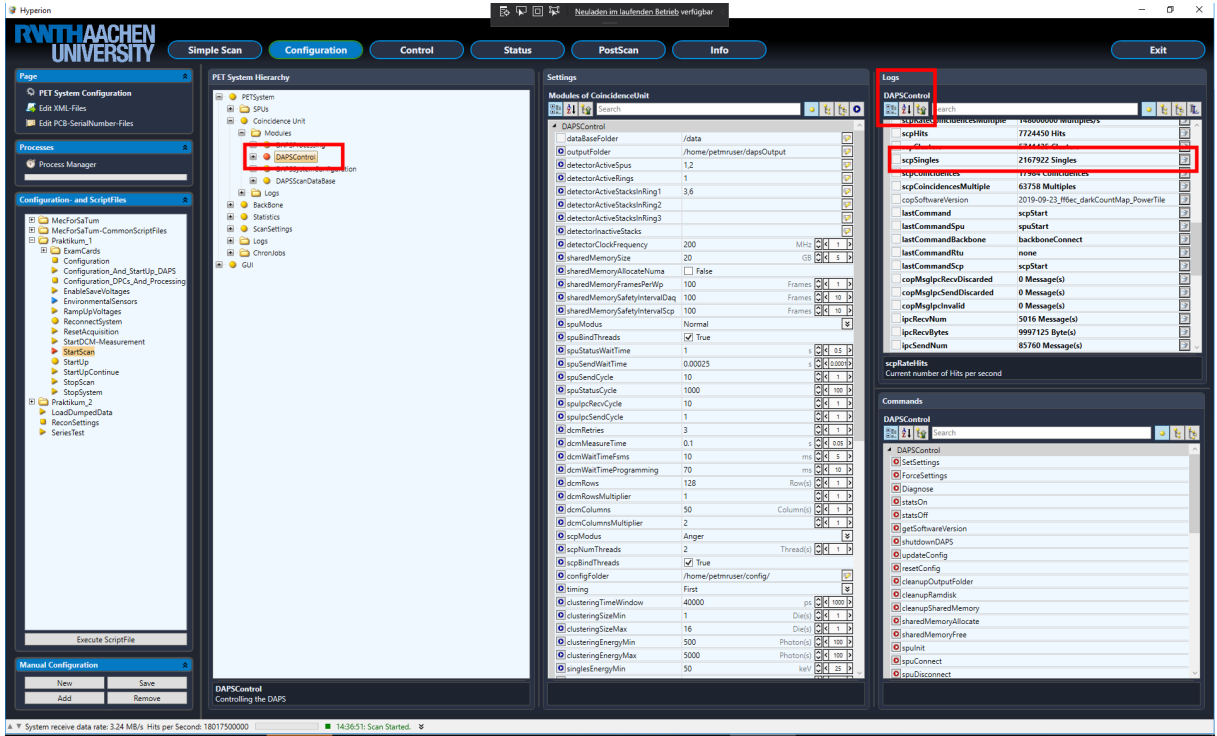


Figure 3.8: Hyperion count rate determination: Interface shown exemplary for singles. Counts can be accessed by selecting the 'DAPSControl' and displaying the counts. The plots can be opened via the button on the right side of the log name.

the save function does not work, switch 'Graph' to 'Text' and copy the values listed to a text file.

- Measure the distances from the source to the detector elements for later estimation of the geometrical sensitivity.
- ### 3.2.7 Energy spectrum
- Go to the 'Control' tab and select the 'Energy spectrum' entry on the left side. Energy histograms for singles and coincidences are displayed on the right side.
 - Reset the histograms and start the measurement to acquire an energy histogram.
 - After the acquisition is finished, save the histograms, check the files and copy them to your USB-stick.
 - Make one measurement without source.



Figure 3.9: Hyperion singles plot: Exemplary plot for the singles. The marked button can be used to save the data. If the save function does not work, switch 'Graph' to 'Text' and copy the values listed.

3.2.8 Timing resolution and determination of source position by Time-of-Flight measurement

First the timing resolution of the detector is determined. To measure the timing resolution, acquire a histogram of time differences for the detected coincidences.

- Reset the measurement and restart it to collect and display the measured time differences.
- Go to the 'Control' tab and select the 'Time difference spectrum' entry on the left side.
- After the acquisition is finished, save the histogram and copy it to your USB-stick.

In the second part you should determine the unknown position of a point source by time-of-flight measurements.

- Move the source to three random positions.
- Go to the timing resolution page and acquire a new histogram of timing differences for each new position. Note, that you have to reset the measurement after moving the source to delete the entries measured at the old position.
- Save the histograms after the measurement, check the file and copy it to your USB-stick.

3.3 Analyzing your data

The data analysis can be done in an arbitrary program.

- Dark count map:
 - Plot the dark count maps in a suitable format.
 - Individual SPADs can be switched off, if they have a high dark count rate. Plot the overall dark count rate of the system against the fraction of inhibited SPADs with highest dark count rate.
- Sensitivity:
 - At the maximum count rate position, calculate the average count rate of singles and coincidences and the uncertainty.
 - Compare the measured values to an estimation based on the geometric efficiency, scintillator dimensions and the activity of the source. In case you find significant differences, discuss by which effects they might be caused.
 - Calculate the sensitivity: To measure the sensitivity, a weak point source is placed in the center position between the detectors. The sensitivity is then determined as the ratio of the coincidence count rate divided by the rate of β -decays of the source.
- Energy spectrum:
 - Plot the energy spectrum in a suitable way and label prominent points.
 - Determine the energy resolution of the PET-scanner and its uncertainty by fitting a Gaussian distribution to the 511 keV photopeak. Reason and discuss what data points you use for the fit.
 - Formulate and, if possible, test potential corrections to the data to improve the analysis. Discuss how the energy resolution of the system can be improved and what are the drawbacks of your suggested modifications.
 - Check the linearity of the energy calibration with the photopeak of ^{22}Na at 1275 keV. Formulate hypotheses why the energy scale might not be accurate at 1275 keV.
- Timing resolution:
 - Plot time difference histogram of the point source at the central position in a suitable way and determine the coincidence resolving time (FWHM) of the PET system by fitting a Gaussian distribution to the time difference histogram.
 - Plot the time difference histogram for the three position. All graphs can be combined to a single plot. Estimate the position of the point source

from this measurements and make an estimation of the positions using the recorded target location.

Bibliography

- [1] Versuch T1: Particle detectors and radiation protection, March 2015.
- [2] Thomas Frach, Gordian Prescher, Carsten Degenhardt, Rik de Gruyter, Anja Schmitz, and Rob Ballizany. The digital silicon photomultiplier. In *2009 IEEE Nuclear Science Symposium Conference Record (NSS/MIC)*, pages 1959–1965. IEEE, 2009.
- [3] H. Malcolm Hudson and Richard S. Larkin. Accelerated image reconstruction using ordered subsets of projection data. *IEEE transactions on medical imaging*, 13(4):601–609, 1994.
- [4] Bernd Jähne. *Digital Image Processing*. Springer Science & Business Media, June 2013. Google-Books-ID: XczuCAAAQBAJ.
- [5] D. Schug, J. Wehner, B. Goldschmidt, C. Lerche, P. M. Dueppenbecker, P. Hallen, B. Weissler, P. Gebhardt, F. Kiessling, and V. Schulz. Data processing for a high resolution preclinical pet detector based on philips dpc digital sipms. *IEEE Transactions on Nuclear Science*, 62(3):669–678, June 2015.
- [6] David Schug. *About the calibration and PET performance of a preclinical PET/MRI insert equipped with digital silicon photomultipliers*. PhD thesis, RWTH Aachen, 2015.
- [7] Lawrence A. Shepp and Yehuda Vardi. Maximum likelihood reconstruction for emission tomography. *IEEE transactions on medical imaging*, 1(2):113–122, 1982.
- [8] Virginia Ch Spanoudaki and Craig S Levin. Photo-detectors for time of flight positron emission tomography (tof-pet). *Sensors*, 10(11):10484–10505, 2010.
- [9] Kenneth M. Tichauer, Yu Wang, Brian W. Pogue, and Jonathan T. C. Liu. Quantitative in vivo cell-surface receptor imaging in oncology: kinetic modeling and paired-agent principles from nuclear medicine and optical imaging. *Physics in Medicine and Biology*, 60(14):R239–269, July 2015.
- [10] B. Weissler, P. Gebhardt, P. M. Dueppenbecker, J. Wehner, D. Schug, C. W. Lerche, B. Goldschmidt, A. Salomon, I. Verel, E. Heijman, M. Perkuhn, D. Heberling, R. M. Botnar, F. Kiessling, and V. Schulz. A Digital Preclinical PET/MRI Insert and Initial Results. *IEEE Transactions on Medical Imaging*, 34(11):2258–2270, November 2015.

- [11] Bjoern Weissler. *Digital PET/MRI for preclinical applications*. PhD thesis, RWTH Aachen, 2016.

A Appendix

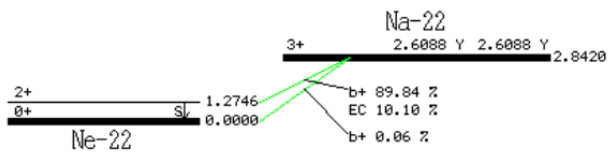
Na-22 decay scheme

22NA B+ DECAY

<http://atom.kaeri.re.kr/cgi-bin/decay?Na-22 EC>

22NA B+ DECAY

Parent state: G.S.
Half life: 2.6088 Y(14)
Q(gs): 2842.0(5) keV
Branch ratio: 1.0



Beta+ ray: total intensity = 89.9

Max.E(keV)	Avg.E(keV)	Intensity(rel)	Spin
1820.0(-)	835.00(23)	0.056(14)	0+
545.4(-)	215.54(21)	89.84(10)	2+

EC: total intensity = 10.1

Gamma ray:

Energy(keV)	Intensity(rel)
1274.53(2)	99.944(14)

P. M. ENDT, *Nuclear Physics A521*, 1 (1990)

Please e-mail to jhchang@kaeri.re.kr for any comment. Thank you.

Figure A.1: Na-22 decay scheme from Korea Atomic Energy Research Center Institute: Table of Nuclides (<http://atom.kaeri.re.kr>)

B Instructions

B.1 Overview of PET-scanner Procedures

1. Basic Start-up:

- Power up the cooling
- Power up the system: Fans and Motors, Backbone, SPUs from Low to High, Bias
- Start Control Software (Hyperion)
- Select the configuration folder 'Praktikum-X'
- Execute 'Start-up' Procedure, wait until finished
- After setup is completed, check that the system operates correctly (Bias voltage about 15V, Temperatures, SPU power supply)

2. Measuring a dark count map (DCM)

- Perform a 'Basic Start-up' (see 1.)
- Ramp up the bias voltage by executing 'RampUpVoltages'
- Check Bias Voltages (about 25 V on all stacks)
- Execute 'StartDCM-Measurement'
- Wait... until finished (Check status)
- Execute the dcm-script on the DAPS to preprocess the dark count maps (done by supervisor)
- Copy files into the dcm Folder on the Control-PC
- Before starting normal measurements, restart the whole system

3. For energy and timing measurements:

- Perform a 'Basic Start-up' (see 1.)
- Execute 'StartUp-Continue' (will ramp up voltages and start clocks)

- Check voltages, frame counters and temperatures on SiPMs under 'Control'
- Wait until the SiPM temperatures are stable
- Execute 'StartScan'
- ... collect data
- Execute StopScan to stop measurement
- If you need to reset the energy and timing histograms execute the ResetAcquisition Procedure

Remarks:

- Do not power up the system without cooling (water cooling for SPU1 and SPIU2 and fan for the backbone).
- Close the dark box before the bias voltage is ramped up (script 'RampUpVoltages' or 'StartUp-Continue')
- Before opening the dark box, lower the bias voltages (script 'EnableSaveVoltages') and check the bias voltages are reduced to about 15V!
- Check bias voltages and IDDA (quench) currents after ramp up and ramp down ('EnableSaveVoltages'). Typical values for ramped down mode are 15 V bias voltage while during ramp up, the bias voltage reaches 25V. IDDA needs to stay below the 100 mA current limiting.
- 'FrameCounters' can be checked, with the 'ReadFrameCounterAtSync' Command under SPUs and sending a sync-pulse from the Backbone ('Modules->SyncPulseCfgUnit')
- Display plots by clicking the 'Change' option and reset the 'measurement interval'. Then, select the parameters that should be displayed.
- Pause histogram plots and refresh them if necessary to avoid memory pile up. The program may crash otherwise.

B.2 Motor controls

B.2.1 Group 1: Dark box setup

The dark box setup has three motorized stages. The stage between the detectors is controlled by the Trinamic Motion Control:

13 - RFS

Reference Search, measures distance between end stops,
the distance in microsteps can be readout by

06 - GAPGetAxis Parameters

Parameter 196 Ref Switch Distance, get amount of steps moved

04 - MVP

Move to positon in microsteps

This setup has two end stops. Thus, the probe holder cannot collide with the SPUs.

The other two stages are controlled via the Thorlabs Kinesis program.

- Home both stages
- Move by clicking 'Move' and insert the desired distance in mm.

B.2.2 Group 2: Open setup with shielded modules

This setup has only two motorized stages. The third stage, which moves the point source up and down, needs to be moved manually.

The program used for the movement between the SPUs is called OWISoft Control (Figure B.1).

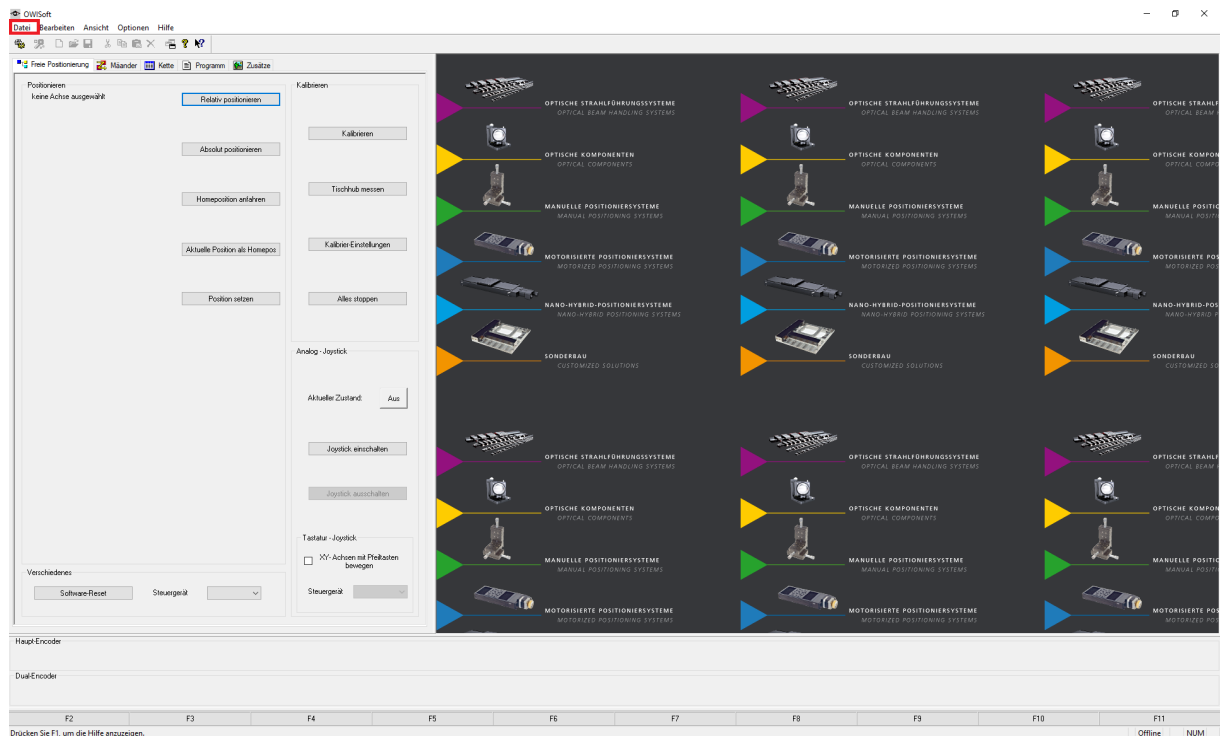


Figure B.1: Owisoft start: Interface for the Owisoft software. Start the initialization of the motor by clicking 'Datei' and selecting the PS10-1.owi.

When opened, an initialization of the motor needs to be done by loading the motor in 'Datei -> PS10-1.owi' and double clicking the red z. A dialog will open for the initialization (Figure B.3). After initialization and start, the movement unit should be changed to steps. Afterwards, the motor can be controlled via the interface (Figure B.2).

The second stage is also controlled using a Thorlabs Kinesis program. The usage is analog to the setup of Group 1.

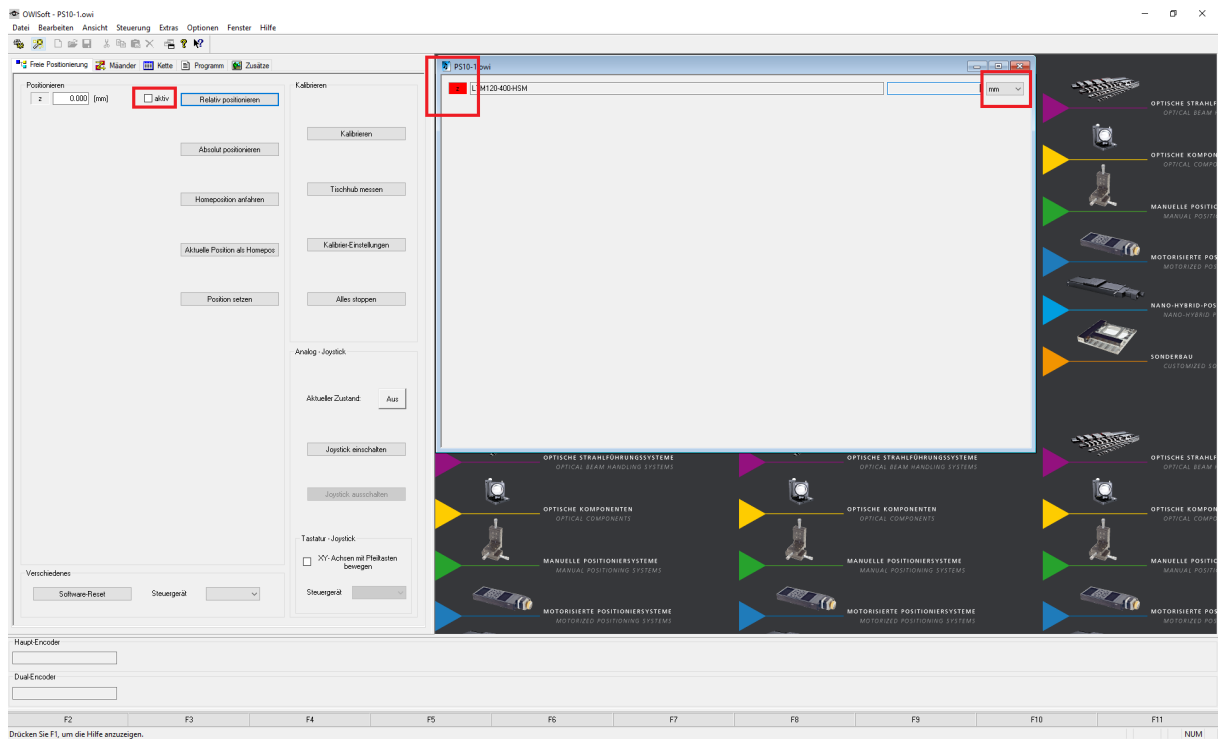


Figure B.2: Owisoft interface: Click on the red z and the initialization dialog will open. This interface will also be used to control the motor. On the right side, the unit can be changed to steps.

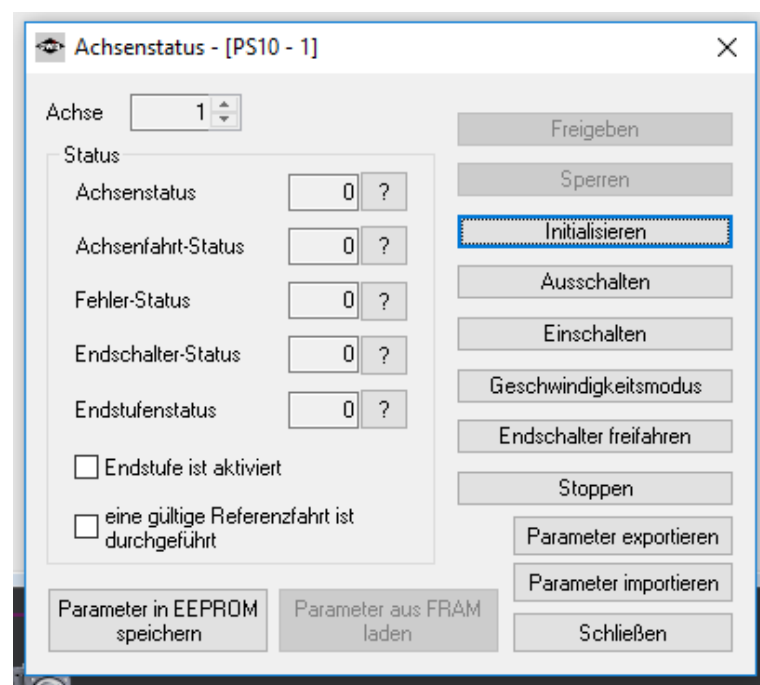


Figure B.3: Owisoft initialization: The motor is initialized using the 'Achsenstatus' dialog. Here, you can initialize, start and stop the motor.